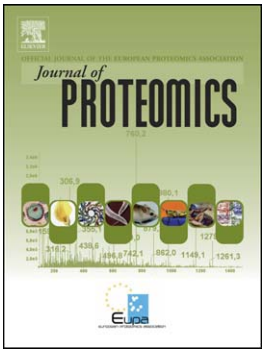

Proteomic investigation of the prefrontal cortex in the rat clomipramine model of depression

Barbara Gellén, Katalin Völgyi, Balázs András Györffy, Boróka Balogh, Zsuzsa Darula, Hunyadi-Gulyás Éva, Péter Baracskay, András Czurkó, István Hernádi, Gábor Juhász, Árpád Dobolyi, Katalin Adrienna Kékesi

PII: S1874-3919(16)30266-4
DOI: doi: 10.1016/j.jprot.2016.06.027
Reference: JPROT 2605

To appear in: *Journal of Proteomics*

Received date: 24 March 2016
Revised date: 17 June 2016
Accepted date: 22 June 2016

Please cite this article as: Gellén Barbara, Völgyi Katalin, Györffy Balázs András, Balogh Boróka, Darula Zsuzsa, Éva Hunyadi-Gulyás, Baracskay Péter, Czurkó András, Hernádi István, Juhász Gábor, Dobolyi Árpád, Kékesi Katalin Adrienna, Proteomic investigation of the prefrontal cortex in the rat clomipramine model of depression, *Journal of Proteomics* (2016), doi: 10.1016/j.jprot.2016.06.027

Proteomic investigation of the prefrontal cortex in the rat clomipramine model of depression

Barbara Gellén[1,2], Katalin Völgyi[1,2], Balázs András Györffy[1,3], Boróka Balogh[1], Zsuzsa Darula[4], Hunyadi-Gulyás Éva[4], Péter Baracskay[1], András Czurkó[1], István Hernádi[5], Gábor Juhász[1,6], Árpád Dobolyi[2], Katalin Adrienna Kékesi[1,7]

[1]Laboratory of Proteomics, Institute of Biology, Eötvös Loránd University, Budapest, Hungary

[2]MTA-ELTE NAP B Laboratory of Molecular and Systems Neurobiology, Institute of Biology, Hungarian Academy of Sciences and Eötvös Loránd University, Budapest, Hungary

[3]MTA-ELTE NAP B Neuroimmunology Research Group, Department of Biochemistry, Institute of Biology, Eötvös Loránd University, Budapest, Hungary

[4]Proteomics Research Group, Institute of Biochemistry, Biological Research Centre, Hungarian Academy of Sciences, Szeged, Hungary

[5]Department of Experimental Neurobiology, Institute of Biology, and Szentagothai Research Center, University of Pécs, Pécs, Hungary

[6]MTA-TTK NAP B MS Neuroproteomics Group, Hungarian Academy of Sciences, Budapest, Hungary

[7]Department of Physiology and Neurobiology, Institute of Biology, Eötvös Loránd University Budapest, Hungary

Keywords: clomipramine treatment, prefrontal cortex (PFC), two-dimensional differential gel electrophoresis (2D-DIGE), macrophage migration inhibitory factor (MIF), depression-like behavior

Abstract

Neonatal rodents chronically treated with the tricyclic antidepressant clomipramine show depression-like behavior, which persists throughout adulthood. Therefore, this animal model is suitable to investigate the pathomechanism of depression, which is still largely unknown at the molecular level beyond monoaminergic dysfunctions. Here, we describe protein level changes in the prefrontal cortex of neonatally clomipramine-treated adult rats correlating with behavioral abnormalities. Clomipramine was administered to rat pups twice daily between postnatal days 8-21, while controls received saline injections. Behavioral tests were performed on 3 months old rats. The proteomic study was conducted using two-dimensional differential gel electrophoresis. We have identified 32 proteins by mass spectrometry analysis of the significantly altered protein spots. The changed proteins are related to several biological functions, such as inflammation, transcription, cell metabolism and cytoskeleton organization. Among the altered proteins, the level of macrophage migration inhibitory factor showed the largest alteration, which was confirmed with Western blot. Macrophage migration inhibitory factor showed widespread distribution and was predominantly expressed in astrocytes in the forebrain of rats which were described using immunohistochemistry. We conclude that neonatal clomipramine exposure induces sustained modification in the proteome, which may form the molecular basis of the observed depression-like behavior in adult rats.

Biological significance

It is known that some of the psychiatric disorders, such as autism, depression or schizophrenia may be at least in part, developmental disorders. We hypothesized that clomipramine treatment in early stage of brain development, which is known to induce depression-like behavior in adult rats, results in pathological distortion in neuronal and glial network development, which can be reflected by the cellular proteome in adulthood. Thus, we performed an unbiased proteomics experiment in adult rats, which were neonatally administered with clomipramine to reveal protein level changes three months after treatment. Many of the identified changed proteins are previously associated with depressive symptoms, e.g., the macrophage migration inhibitory factor (MIF), the level of which showed the largest alteration among the identified proteins. Based on our data, we suggest that neonatal clomipramine treatment is a reliable model to study the developmental effect of psychoactive drugs applied in the sensitive early phase of brain development. Furthermore, our findings support the idea that the alteration of early development of the brain induced by antidepressant treatment could result in sustained pathological changes in the cellular phenotype in the prefrontal cortex leading to depression-like behavioral symptoms.

1. Introduction

Depression affects millions of people worldwide, as it was rated the fourth leading disabling condition in the year 2000 [1], and it is predicted that it would be the second by 2020 [2]. According to the 5th edition of Diagnostic and Statistical Manual of Mental Disorders (DSM-5), major depressive disorder (MDD) or clinical depression can be diagnosed if the patient meets five of nine symptoms for at least 2 weeks long [3]. However, we still lack the proper molecular biomarkers to precisely diagnose the disease. Although effective treatments are available, the problem is that not all patients respond to them, most

likely because depression is a molecularly heterogeneous disease. Still, most of the obtainable and effectively used medications are based on elevation of monoamine levels in line with the monoamine hypothesis of depression [4-6]. It is unknown, however, why mood improving effects of the medications appear only after several weeks of treatment, and depression cannot be initiated by reducing the levels of the monoamines in a healthy subject [7]. A modified hypothesis has been postulated that antidepressant medication may alleviate depression through the desensitization of 5-HT1A, 5-HT3 and 5-HT7 serotonin receptors [4, 8].

In contrast to early theories which emphasize the exceptional significance of the monoamine systems, depression is actually considered to be the result of complex interactions between thousands of genes and multiple environmental risk factors. None of them alone can cause depression. Recently, a hypothesis of depression emerged implicating the altered neuroplasticity in the disease. Depressed patients show evidence of impaired neuroplasticity and antidepressant medications enhance neuroplasticity at both the molecular and the cellular level [9]. There is also an inflammatory hypothesis of depression, which is proposed by the observation that elevated levels of proinflammatory cytokines are present both in blood plasma, and in the cerebrospinal fluid during depressive states in patients [10, 11]. Furthermore, sickness feeling after viral or bacterial infection has similar symptoms as depression suggesting similarities in their molecular background [12, 13]. However, the alterations may not be equally located in the brain. The peculiar role of the prefrontal cortex (PFC) in depression has been suggested based on structural and functional neuroimaging [14] and lesion studies [15, 16].

It has been established that neonatal administration of the tricyclic antidepressants in rodents provides a well-characterized animal model of major depression. Neonatal rat pups, chronically treated with clomipramine or the selective serotonin reuptake inhibitor (SSRI) citalopram, demonstrated persistent changes in behavior in adulthood (which phenomenon

was named "neonatal antidepressant exposure syndrome" (NADES)) including characteristics of depression-like behaviors and changes in sleep pattern of adult rats [17-20]. In the clomipramine model, altered expression of 5-HT1A receptor was recently demonstrated, which is in accordance with the monoamine hypothesis of depression [21]. It was also shown that mammalian target of rapamycin (mTOR) signaling is also compromised in clomipramine rat model in accordance with the altered neuroplasticity hypothesis of depression [22]. In addition, we previously demonstrated that neonatal clomipramine treatment aggravated the depression-like symptoms in WAG/Rij rats (a genetic rat model of absence epilepsy), and decreased their epileptic activity [23]. Although, the neurobiological processes behind NADES are unknown, antidepressant administration of rats during their highly-sensitive brain development period could model the long-term detrimental effects of depression in general, and specifically the maternal antidepressant medication on developing fetuses or neonate children [24]. Therefore, we addressed the question whether there is a detectable phenotype modifiation in cells of the PFC in the clomipramine model of depression [15, 16, 25, 26].

2. Materials and methods

2.1. Animals

Wistar rats (Toxi-Coop, Budapest, Hungary) were housed under standard laboratory conditions (12:12 h light:dark periods, light was on from 8.00 am to 8.00 pm) at a constant temperature of 22 ± 2 ºC. Food and water were supplied *ad libitum*. The care and treatment of all animals conformed to Hungarian Act of Animal Care and Experimentation (1998, XXVIII) and to the guidelines of the European Communities Council Directive, 86/609/EEC as well as with local regulations for the care and use of animals for research.

2.2. Experimental design

Six litters of rats were used for the experiments. We have taken account the mortality caused by the clomipramine treatment, therefore on postnatal day (PD) 8, we randomly assigned 3-4 female pups per litter for chronic clomipramine treatment (CLO) and the rest of the females were received vehicle (physiological saline solution) injections (control, C). From PD 8 to 21 of age, all experimental animals were treated twice a day (between 8.00-9.00 a.m. and 6.00-7.00 p.m.) as follows: CLO-rats received clomipramine (20 mg/kg, subcutaneously) (Sigma–Aldrich, Germany) dissolved in 700 µl saline and the control group received saline in the same volume. The weight of animals was monitored throughout the chronic clomipramine administration. Surprisingly, there was no significant alteration between the control and clomipramine treated groups. At 30 days of age, offspring were separated from their mothers. Three-four gender-matched rats per cage were housed together until the behavioral tests. The gender-related differential responses to clomipramine treatment in rat model were investigated by behavior tests before [27]. Kokras et al. found relevant behavioral responses and elevated serotonin turnover rate in both genders. However, they revealed that the effect of antidepressant administration was more pronounced in females. Based on these findings female rat pups were used in our experiments.

2.3. Forced swim test

We used the forced swim test (FST) procedure to test the depression-like behavior of rats. The FST is a widely accepted, frequently used test for investigating depression-like behavior in rodents [28, 29]. It could have been very useful to test anhedonia in addition to the learned helplessness and correlate the two trait signs of depression-like behavior, without the necessity to use additional tests which could pose significant stress affecting the subsequent molecular experiment. The FST procedure involves the scoring of active (swimming and struggling) or passive (immobile floating) behaviors while the subjects are placed in a water-

filled cylinder from which escape is not possible. The latency and duration of passive behavior called here floating are informative on the learned helplessness of the animals [30].

A total of 20 rats (n = 10 in each group) at 3 months of age (270-300 g) were used in the experiments. The apparatus used in the present study was a clear rectangular glass cylinder with dimensions of 30x30x50 cm (width x depth x height) which was filled with lukewarm water (26-28 °C) to the height of appx. 20 cm, thus the animal could not comfortably rest his hindlegs at the bottom. The apparatus was put in sound attenuated, dimly lit experimental room with controlled ambient temperature conditions (24 °C). Each test sessions were held in the mornings between 9:00 am and 12:00 am. Test sessions were lasted for 5 min and were repeated three times, once on each of the three consecutive test days to ensure the stability of the observed trait behavioral signs. The cylinder was cleaned between rats and was emptied and re-filled when required during the test sessions. All subjects were tested in the same order. One hour before the test sessions begun, the animals were transported to the test room on a rack, and were accommodated in an enclosure close to the testing apparatus. The FST test sessions were continuously video-recorded from the side of the cylinder. Video recordings were scored off line by two independent raters. Inter-rater reliability (measured with Cohen's kappa) values for the three dependent variables in the two conditions fell in the fair-to-good range (between 0.61 and 0.7) [31].The mean of the scores were used as processed data. Latency to reach passive floating behavior (immobility) was defined as the time at which the rat first initiated a stationary posture that did not attempt to escape. In this characteristic posture, the forelimbs were motionless and tucked toward the body with the head kept out of the water. To qualify as immobility, floating had to be present for at least 2 s. In addition to immobility latency data, the total time spent with the passive floating behavior was also computed. Statistical tests were performed using R for Windows 3.2.3 (R Core Team, 2016. R: a Language and Environment for Statistical Computing. R

Foundation for Statistical Computing, Vienna, Austria. http://www.R-project.org.) Shapiro-Wilk test was performed to check normality of variables. Because non-normal distribution was found ($p<0.05$) we used Brunner-Munzel test of the R package "lowstat" v.3.0."

2.4. Proteomics experiment

2.4.1. Preparation of tissue samples and the 2-D DIGE method

One week after the behavioral tests, rats (6 control and 6 CLO treated) were deeply anaesthetized with intraperitoneal urethane administration. Their brains were quickly removed from their skulls and were placed in dry ice-cooled artificial cerebrospinal fluid. Prefrontal cortices were dissected immediately and the samples were stored at -80 °C.

The proteomic analysis was performed using two-dimensional differential gel electrophoresis (2-D DIGE) Minimal Dye Labeling method. All equipment, materials and softwares were supplied from GE Healthcare, Little Chalfont, UK. The detailed 2-D DIGE protocol has been described in our earlier study [32]. In briefly, brain samples were homogenized and their protein concentrations were determined using a 2-D Quant Kit. Samples, containing 50 µg protein amount from three CLO and three C rats were labeled with Cy3 and Cy5 dyes randomly, and the other half of the samples were labeled conversely. The reference sample (pooled internal standard, which comprises equal amounts of protein from all biological samples in the experiment) was labeled with Cy2 dye. The differently labeled samples from randomly paired CLO and C rats and equal amounts from the reference sample, were multiplexed and subjected for electrophoresis. Samples were dissolved in isoelectric focusing (IEF) buffer containing ampholytes and rehydrated passively onto 24 cm NL IPG strips overnight. After rehydration, the IPG strips were subjected to first dimension IEF for 24 h to attain a total of 80 kVh. Subsequent to IEF, the gels were equilibrated in reducing conditions, then the proteins were carbamidomethylated for 20-20 min, respectively. After

equilibrations, the IPG strips were loaded onto 10% polyacrylamide gels (24×20 cm), and SDS-PAGE was conducted at 2 W/gel for 1 h and at 12 W/gel for 3 h in the second dimension using an Ettan DALT Six System. Following electrophoresis, gels were scanned in a Typhoon TRIO+ scanner using appropriate lasers and filters with the photomultiplier tube was biased at 600 V. The gel images were visualized using the Image Quant software. Quantitation of fluorescence intensities of the protein spots and statistical analyses (independent, two-tailed Student's *t*-test) were performed using the DeCyder 2-D Differential Analysis Software package (GE Healthcare, Little Chalfont, UK). The used fluorescent labeling technology and software analysis enable identification of strikingly low-level protein abundance differences (less than 10%) with more than 95% confidence [33]. Therefore, the cut-off of ± 1.1-fold change in fluorescence intensity of matched protein spots between experimental groups was applied in the current study.

For the identification of proteins in spots of interest, preparative 2-D gel electrophoresis was carried out separately using a total of 800 µg of proteins. Proteins were stained with Colloidal Coomassie Brilliant Blue G-250 (Merck Millipore, Darmstadt, Germany). The significantly altered protein spots were manually excised from the preparative gel and were stored in 1% acetic acid solution until the mass spectrometry (MS) analysis.

2.4.2. Protein identification using mass spectrometry (LC-MS/MS)

Excised protein spots were in-gel digested for MS-based protein identification, using the protocol provided by the UCSF Mass Spectrometry Facility (University of California, San Francisco, San Francisco, CA, USA) and, which is available online at: http://msf.ucsf.edu/protocols.html. Briefly, after dithiothreitol reduction and iodoacetamide alkylation, the proteins were digested with trypsin (sequencing grade modified trypsin from pig pancreas, Promega, Madison, WI, USA). Peptides were subjected to LC-MS/MS analysis

on an LCQ-Fleet iontrap mass spectrometer (Thermo Fisher Scientific, Waltham, MA, USA), on-line coupled with a nano-Acquity HPLC system (Waters Corporation, Milford, MA, USA). Five µl out of the 10 µl peptide extracts were injected to the nano-HPLC system, using a trap column (Symmetry C18, 0.18×20 mm, 5 µm, Waters Corporation) and analyzed on a BEH300 C18 1.7 um (0.1 × 100 mm) nanoAcquity UPLC Column (Waters Corporation), using a gradient elution (10-40 % of B in 30 minutes; B: 0.1 % formic acid in acetonitrile; A: 0.1 % formic acid in water). MS data were acquired in a data-dependent mode, using triple play method. Each survey scan was followed by zoom scans and collision-induced dissociation (CID) scans (normalized collision energy: 35) of the three most abundant multiply charged precursor ions. Dynamic exclusion was set to 30 s. Mascot Distiller software (version 2.2.1.0, Matrix Science Inc., London, UK) was used to generate the MS/MS peak list files from the raw data, and ProteinProspector (version 5.3.0.) search engine for database search. The parameters were set as follows during the search in the latest UniProt database (http://www.uniprot.org, Swiss Institute of Bioinformatics, Switzerland). The searching was conducted with settings as follows: taxonomy: *Rattus norvegicus*; enzyme: trypsin (two missed cleavage sites were allowed); fixed modifications: carbamidomethylation; variable modifications: acetylation (protein N-terminus), Gln to pyro-Glu (N-terminus Q), oxidation; peptide mass tolerance: ± 0.6 Da; fragment mass tolerance: ± 1 Da. Proteins, identified at least with two unique peptides were considered as valid hits.

2.4.3. Functional clustering of identified proteins and bioinformatic analysis

Based on the UniProt database and on an extensive literature search, functional clustering of proteins was performed. For detailed protein interaction modeling analysis, Pathway Studio 9.0 software (Ariadne Genomics, Inc., Rockville, MD, USA) was used. The pathways were created based on expression regulation between the proteins. We selected

common regulator proteins that have minimum 3 relations with significantly changed proteins from the experimental results and connected with MIF for further analysis. In the common target pathway we included targets which have relations with MIF. The created protein network model was manually verified using thorough literature mining.

2.5. Western blot

The proteins of homogenized PFC tissues were precipitated using chloroform and methanol [34]. Subsequently, samples (n = 4 in each group) were resuspended in lysis buffer, and were assayed for protein concentration using 2-D Quant Kit. Thirty-five micrograms of proteins were separated using Tricine-SDS-polyacrylamide gel electrophoresis on 15% polyacrylamide gels, and then proteins were transferred to Hybond-LFP polyvinylidene difluoride (PVDF) transfer membranes (GE Healthcare). The gels were stained with Coomassie Brilliant Blue R-250 (Merck Millipore) and the total protein amount was precisely determined for each lane based on their densities. The membranes were blocked with 5% bovine serum albumin (BSA) in Tris-buffered saline with 0.1% Tween-20 (TBS-T), and incubated with rabbit anti-MIF primary antibody (Abcam, Cambridge, UK, cat. number: ab7207) in 1:1,500 dilution in TBS-T, overnight. Subsequently, the membranes were extensively washed in TBS-T, followed by incubation with ECL Plex Cy5-conjugated anti-rabbit IgG secondary antibody (1:2,500 dilution, GE Healthcare). After consecutive washing steps in TBS-T, and then in TBS, the protein bands on the blots were visualized using a Typhoon TRIO+ scanner. Fluorescence intensities were quantified using ImageJ software (NIH, Bethesda, MD, USA). Fluorescence intensity values were normalized to the densitometric values of their corresponding Coomassie Brilliant Blue R-250-stained lanes, which eliminated errors due to unequal protein loading. Differences between the normalized

values from CLO and C samples were statistically analyzed using independent, two-tailed Student's *t*-test in OriginPro 9.0 (OriginLab Corporation, Northampton, MA, USA).

2.6. Double immunohistochemistry labeling for MIF with NeuN and S100

The removed brains (n = 4 in each group) were transferred to phosphate buffer (PB) containing 20% sucrose for 2 days for cryoprotection and were frozen before sectioning. Serial coronal brain sections were cut at 40 μm on a freezing microtome. Sections were collected in PB containing 0.1% sodium-azide and stored at 4 ºC. Free floating tissue sections were processed for immunolabeling. First, the sections were treated with 3% BSA, 0.5% Triton-X 100, 0.05% sodium azide dissolved in PB, followed by washes in PB. Every fourth tissue section was immunolabelled with mouse anti-NeuN as a marker of neurons (1:500 dilution; Millipore, Billerica, MA, USA, cat. number: MAB377) or mouse anti-S100 as a marker of astrocytes (1:10,000; Sigma-Aldrich, cat. number: S2532) for 24 h. Subsequently, Alexa Fluor 594 donkey anti-mouse secondary antibody (1:500; Molecular Probes, Eugene, OR, USA) was applied for 1 h. All of the sections were then incubated with rabbit anti-MIF (1:40; Abcam) for 48 h, followed by incubation with biotinylated donkey anti-rabbit secondary antibody (1:1,000; Jackson Immunoresearch, West Grove, PA, USA) for 1 h and with ABC complex (1:500; Vector Laboratories, Burlingame, CA, USA) also for 1 h. Sections were subsequently incubated with FITC-tyramide (1:8,000) and H_2O_2 in 0.05 M Tris-hydrochloride buffer, pH 8.0, for 6 min. After washes, the sections were mounted on slides and coverslipped with Aqua-Poly/Mount medium (Polysciences Inc., Warrington, PA, USA).

2.7. Microscopy and image processing

The sections were examined using an Olympus BX60 light microscope in both dark-, and bright-field modes. Images were captured at 2,048 x 2,048 pixel resolution using a SPOT

Xplorer digital CCD camera (Diagnostic Instruments, Sterling Heights, MI, USA), equipped with a 4x objective. The contrast and sharpness of the images were adjusted using the ‘‘levels’’ and ‘‘sharpness’’ commands in Adobe Photoshop CS 8 (Adobe Systems, San Jose, CA, USA). The confocal microscopy examination was conducted with a Nikon Eclipse E800 microscope (Nikon Corporation, Tokyo, Japan) equipped with Bio Radiance 2100 Laser Scanning System (Bio-Rad Laboratories, Hercules, CA, USA) using a 63x objective. Images were captured at 1,024 x 1,024 pixel resolution with 2 μm optical thickness. Full resolution of the images was maintained until the final figures were assembled, at which point, the images were adjusted to a resolution of 300 dpi.

3. Results

3.1. Depression-like behavioral effect of neonatal clomipramine treatment

Within the FST session CLO rats had a higher tendency (as compared to controls) to make only those movements necessary to keep their heads above water, and showed increased immobility (floating) as a sign of depression-like trait behavior. The rats from the C group spent 88.1 ± 8.0 s with floating, 97.9 ± 8.1 s with swimming, and 114.0 ± 8.9 s with struggling. The animals in the CLO group spent 131.5 ± 9.1 s with floating, 81.0 ± 8.1 s with swimming, and 87.5 ± 7.4 s with struggling (Figure 1). According to the statistical analysis, the average time spent with floating was significantly elevated in the CLO group ($p < 0.001$) in comparison with the C group, while the average time spent with struggling was significantly reduced due to the treatment ($p < 0.05$).

3.2. Protein level alterations

The 2-D DIGE proteomics technology was used to investigate the differences in the pattern of protein level changes in the PFC of neonatally clomipramine-treated adult rats in

comparison with controls. After exclusion of false spots via rigorous manual validation, 927 spots were accepted on the gels, of which 33 were significantly changed ($p < 0.05$) with higher than ±1.1-fold difference between the control and treated groups. A representative image of a gel is shown in Figure 2. Twenty-four of these spots were reliably excised from the preparative gel for further protein identification. The HPLC-MS/MS analysis revealed a total of 32 different proteins in the spots (Table 1 and 2, Supplementary Table 1). Out of them, 18 showed increased, while 14 showed decreased abundance levels in the CLO in comparison with the C group. Among the identified proteins, aconitase 2 (ACO2) and dihydropyrimidinase-related protein 2 (DPYSL-2) were found in more than one spots, which could be explained by their potential post-translational modifications, their cleavage by enzymes or the presence of their different protein species.

3.3. Clustering of the altered proteins

Based on the functional analysis of the altered proteins, different processes of the cellular metabolism (such as tricarboxylic acid cycle, phosphocreatine, carbohydrate, glucose and purine nucleoside metabolism) were affected the most by the clomipramine treatment (Figure 3). In addition, significant changes were observed in the levels of proteins, which play essential regulatory role in transcription and translation of proteins, cytoskeletal organization, regulatory functions such as differentiation and ion homeostasis, stress response (chaperones), proliferation, and immune response.

According to their localization, most of the identified proteins are present in the cytoplasm. Others could be found in the nucleus, membrane, mithochondria, extracellular space or in various combinations of the above-mentioned cellular components (Figure 4).

3.4. Pathway analysis

The result of the pathway analysis is shown in Figure 5. Common expression regulator analysis has revealed 10 proteins connected to MIF (Figure 5A). Eight other proteins with changed levels (DPYSL2, GAPDH, GSTA2, HOMER1, HSPA8, PGK1, TPI1, and TXN) are also connected to these common regulators. Based on our analysis, MIF has 27 common targets, which are also connected to at least one other altered protein (Figure 5B). Among the changed proteins, GAPDH, HSPA8, PGK1, and TXN are connected to one or more targets of MIF. Interestingly, TXN regulates 23 proteins from the 27 MIF-regulated ones.

3.5. Confirmation of the increase in the level of MIF

The change in the level of MIF described in the proteomics experiment was validated using Western blot technique. This protein was chosen because it showed the largest difference between the two experimental groups (1.65-fold elevation in CLO rats) in the proteomics investigation (Table 1). The Western blot experiment verified our proteomic result, because the alteration in the level of MIF was 1.63 ± 0.52-fold increase ($p < 0.05$) in the CLO group in comparison with the controls as shown in Figure 6. In the Western blot analysis, the detected protein band at approximately 12.5 kDa corresponds to the monomeric form of MIF.

3.6. Localization of MIF in the PFC

Immunolabeled cell bodies as well as proximal processes appeared in the PFC. The distribution of the labeled cells was similar in all parts of PFC. On the other hand, layer-specific differences were observed in the density of labeled cells, because MIF-immunoreactive (MIF-ir) cells were particularly abundant in layer I. This distribution resembled to that of the astrocytes and was indeed very similar to that of S100-ir cells (Figure 7). Double immunolabeling revealed that MIF co-localized mainly with astrocytes, and in

fact, most of the S100-ir cells were MIF-positive as well. In addition, a few NeuN-positive neurons were also positive for MIF, however, these particular cells accounted only for a very low portion of the NeuN-ir neurons. Accordingly, the general distribution pattern of MIF-ir and NeuN-ir cells was visibly different, for example, neurons are scarce in layer I where MIF-ir cells were most abundant. The neurons double labeled with MIF and NeuN were relatively evenly distributed. Furthermore, immunohistochemistry demonstrated no difference in the distribution of MIF-ir cells between the CLO and C groups.

4. Discussions

We report here on the changes in molecular phyenotype in prefrontal cortical cells of rats subjected to neonatal clomipramine treatment to induce depression-like symptoms in adulthood. The detected depression-like behavior in the treated rats confirmed the previously reported behavioral effects, a pronounced immobility in the FST [35, 36]. The amount of proteins with altered levels in the adult PFC in response to neonatal clomipramine treatment proves that the treatment induced long-term alterations at the level of the proteome. The altered proteins belong to several functional groups suggesting that different cellular processes are involved in the neonatally applied clomiparamine model of depression. It has to be noted that the observed changes are not necessarily induced by clomipramine treatment directly. Rather, clomipramine initiated cellular processes in early development of the neonatal brain, which probably gradually developed to the observed changes in adult mature phyenotype of PFC cells.

4.1. Energy metabolism

Four proteins with significantly altered levels can be linked to glycolysis. The level of galactokinase (GALK1) was higher in the CLO than in the C group. This enzyme converts

galactose to galactose-1-phosphate, therefore, the latter can enter the process of glycolysis. Additional steps in glycolysis might be also particularly important because the levels of different enzymes, involved in the glycolytic process, were altered. The level of triosephosphate isomerase (TPI1) was increased, while that of glyceraldehyde-3-phosphate dehydrogenase (GAPDH) and phosphoglycerate kinase (PGK1) have been reduced in the CLO group. These findings strongly suggest that depression-like symptoms in this animal model are linked to changes in the metabolic activity of the PFC.

Reduction in the level of the mitochondrial aconitase 2 (ACO2) protein has been found in two spots, in addition to the decrease in the amount of pyruvate dehydrogenase (PDHA1). These proteins play pivotal roles in the tricarboxylic acid cycle. The expression of these metabolic proteins have been found to change in rats following learned helplessness and antidepressant treatment [37]. An increase in the level of malate dehydrogenase (MDH1) in our experiment is also in agreement with the results of a previous proteomic investigation conducted on MDD patients [38].

The level of NADH dehydrogenase (ubiquinone) Fe-S protein 8 (NDUFS8) was reduced, while that of ATP synthase (ATP synthase, H^+ transporting, mitochondrial F1 complex, gamma polypeptide 1) (ATP5C1) was increased upon the treatment. These two proteins are linked to energy production and restoration through their function in oxidative phosphorylation. Thus, their altered level in the CLO depression model suggests that energy production may be affected in depression. Indeed, chronic administration of the tricyclic antidepressant imipramine in rats resulted in altered respiratory rates and increased ATP synthesis in brain mitochondria [39]. The significance of the correlation between mitochondrial functions and MDD has been emphasized recently [40, 41], and our results are consistent with this correlation.

The level of creatine kinase b (CKB), another protein involved in energy homeostasis, was elevated in the CLO group. Notably, CKB produces phosphocreatine, an important mobilizable energy supply for the brain. The literature related to association between CKB levels and depression is controversial in some aspects. The increase in the level of CKB in the serum of non-psychotic major depression patients had been revealed previously in comparison with other types of depression syndromes [42], and in the serum of bipolar disorder patients in manic phase [43]. The activity of this protein was also increased in the PFC of rats after chronic treatment with the antidepressant paroxetine [44]. On the other hand, both isoforms of creatine kinase have been found to be downregulated in the dorsolateral prefrontal cortices of bipolar disorder patients [45].

In addition, the level of CKB in serum has been used as a biomarker to differentiate between psychotic and non-psychotic depression patients on a molecular basis [42].

Glutathione transferase (GST) the level of which was increased following to clomipramine treatment acts as a coenzyme and antioxidant. Of importance, the PFC of schizophrenia and MDD patients showed a reduced level of a protein species of GST indicative of a lowered detoxifying capability and an increased susceptibility to oxidative damage and suggesting GST protein as target for mood stabilizers [46]. Accordingly, it has been demonstrated that particular mood-improving treatments elevate the expression level and activity of GST [47, 48].

Alterations in the metabolic activity related to depression have been described in previous studies in other depression models as well [49, 50]. This correlation was supported by our findings, as we found alterations in a number of novel and previously described metabolic protein in relation to depression.

4.2. Cytoskeleton

F-actin-capping protein subunit beta (CAPZB) showed elevation in CLO group, which protein's function is capping of the actin filaments, and thereby, the regulation of the actin cytoskeleton. Reduction of DPYSL2, a protein that affects cytoskeletal organization and axon guidance, was also found in three different spots. The levels of two other proteins, septin 11 (SEPT11) and translationally controlled 1 tumor protein (TPT1), involved in cytoskeleton regulation, were reduced. These protein level alterations suggest modification of the microfilament structure, which is strongly related to synaptic plasticity. Indeed, one of the recent trends in psychiatric disease research is the investigation of associations with synaptic and cytoskeletal plasticity [51, 52]. Alteration in the expression of cytoskeletal proteins, e.g., β-actin was reported by the influence of stress or antidepressant medication [53]. Elevation in the levels of tubulin protein species was found, which proteins are main components of the cytoskeletal system. The difference between the positions of tubulin isoforms identified in our study (at the ~30-40 kDa range) and their theoretical molecular weights at ~50 kDa suggests that certain posttranslationally modified forms of the tubulins have been found. The posttranslational modification of the alpha form was also observed previously, which could play a pivotal role in stress-related mechanisms through regulating neuronal plasticity as studied in the hippocampus [54]. The link between stress-induced microtubule changes and depression is also strengthened by the fact that acute and/or chronic antidepressant treatment can affect the microtubular dynamics [55]. Interestingly, treatment with the antidepressant escitalopram decreases the dynamics of microtubule system in the hippocampus [56, 57]. Our results in CLO animals, and the above-mentioned previous reports suggest cytoskeletal disturbances behind depression-like behavior [58]. Furthermore, we identified several proteins, which could be involved in the cytoskeletal rearrangement in depression.

4.3. Transcription and translation

Several proteins involved in transcription and translation have been implicated in depression diseases [9]. In our experiment, transcription elongation factor b (TCEB2) showed an elevated, while eukaryotic translation initiation factor 4H (EIF4H) and the large ribosomal protein (RPLP2) showed a reduced level as late results of the neonatal antidepressant treatment. Our results suggest that these three proteins may be involved in regulation of altered gene expression in depression, which is their first implication in that regard.

4.4. Stress response

The heat shock cognate 71 kDa protein (HSPA8) showed elevation, while the stress-70 protein (HSPA9) showed reduction in their levels in the CLO rats. The HSPA8 has a function in RNA splicing, and also in protein folding, as does HSPA9, which also plays a role in the regulation of cell proliferation. From the heat shock protein family, HSP70 was recently correlated to depression in patients with ulcerative colitis, and suggested to be used as a biomarker of the psychosomatic features of this disease [59]. Furthermore, the HSP70 coding genes were associated with the response to antidepressants in mood disorders [60]. In a mouse model of depression, genes related to mitochondrial unfolded protein response, such as HSPA9 were found to be correlated with depression-like behavior [41]. Stress-induced-phosphoprotein 1 (STIP1) acting on folding of proteins, was altered in our study, such as in a previous study on depression patients [61]. The level of two proteins, implicated in response to oxidative stress, namely thioredoxin (TXN) and homer 1 (HOMER1), were also elevated in our model, which is the first evidence for their potential involvement in depression. Overall, the results, together with previous literature data suggest an altered cellular stress in some brain cells during depression.

4.5. Common regulators and targets of the significantly altered proteins in CLO rats

Two pathways were built, comprising the altered proteins, based on the analyses performed using Pathway Studio. According to the first pathway, focusing on the common expression regulators of the altered proteins (Figure 5A), we can conclude that certain cytokines have roles in connecting the altered proteins to each other. These cytokines are interleukin-1 beta (IL1-β), which links three of the proteins, namely MIF, glutathione S-transferase alpha-2 (GSTA2), and TPI1 and tumor necrosis factor (TNF-α) by regulating MIF, TXN, GAPDH and also HSPA8 expression. This finding emphasizes that some cytokines might represent future drug targets in the development of novel antidepressant medication as highlighted previously [10, 62, 63]. Among other common regulators, some general protein expression regulators were also found, such as cyclic AMP-responsive element-binding protein 1 (CREB1), transcription factor Sp1 (SP1), CCAAT/enhancer-binding protein alpha (CEBPA) and mitogen-activated protein kinase 1 (MAPK1). It is also suggested that proteins implicated in basic cell metabolism, such as insulin (INS) could have affected the expression of the changed proteins.

The second pathway was constructed on the basis of common targets of the altered proteins (Figure 5B). Interestingly, there were few common targets of the altered proteins. Therefore, we focused on MIF, a protein, which showed the largest increase in the CLO group. MIF shared a large number of targets with thioredoxin (TXN), in addition TXN can regulate the expression of MIF, as well. These findings indicate that MIF and TXN participate in common regulatory functions. Specifically, both contribute to the expression changes of 14 different chemokines and cytokines. This observation underlie again the important roles of members of the immune system in our animal model of depression. The second largest group of proteins, which are regulated by both MIF and TXN, have functions in apoptosis and / or cell growth (n = 11). In addition to TXN, MIF also has some common targets with PGK1 as

both regulate matrix metalloproteinases (n = 2) functioning in a broad range of biological processes.

4.6. MIF, hypothalamic-pituitary-adrenal axis and inflammation

The MIF showed the largest change, a 1.65-fold increase among the altered proteins in the CLO group, which was also validated by western blotting. Macrophage migration inhibitory factor is a proinflammatory cytokine, with functions in inflammation, apoptosis, metabolic and neuroendocrine processes [64]. This protein can be linked to depression as part of the inflammatory hypothesis of the disease, which comes from the finding that in depressive states, elevated levels of proinflammatory cytokines can be measured both in the plasma and cerebrospinal fluid [10, 11], and that anti-inflammatory treatments can exert antidepressant effect [65]. Interestingly, others also associated MIF level alterations with depressive and anxiety symptoms [66-68]. In addition, a 1.4-fold increase was described in the levels of MIF in the serum of the high-depressive symptoms group compared to the low depressive group[67]. Furthermore, MIF also reduces glucocorticoid (GC) sensitivity, which has been associated with dysphoric states including depression [69-71]. The ability of cytokines to decrease GC sensitivity in immune cells has been described for MIF and interleukin-1 *in vitro*, and has been only shown for MIF *in vivo* [67, 72, 73]. These findings could be linked to the functions of the hypothalamic-pituitary-adrenal axis (HPA) as animals of the clomipramine model of depression show cortisol hypersecretion as a consequence of a hyperactive HPA axis [74]. Studies from as far as the 1990's implicate the dysregulation of the HPA axis and the dysfunction of the negative feedback loop of the HPA axis in depression [75]. In the frontal cortex, elevated corticotropin-releasing factor (CRF) level in depression caused a reduction in the CRF receptor binding sites [76], further supporting the link between depression and abnormal function of the HPA axis. Since we found only one cytokine, which

changed significantly among the altered proteins, MIF could even be one of the main mediators of the HPA axis dysfuntion observed in the clomipramine model of depression. Of interest, MIF could also regulate a plethora of cytokines as it has been revealed in our pathway analysis (Figure 5B). It is possible that clomipramine acutely elevated the levels of cortisol or induced anti-inflammatory cytokine secretion (e.g., interleukin-10 in the serum), as described before [77], and our finding on the elevated level of MIF represents a long-term compensatory mechanism against the triggered changes by adulthood.

Macrophage migration inhibitory factor has a wide distribution in the adult rat brain, as described by Bacher *et al.*, 1998 [78]. Strong immunostaining signal was detected previously throughout the brain (e.g., in the pons, cerebellum, hippocampus, and axons of neurons in the supragranular layer of the cortex) and also in a diffuse pattern in the cortex, which predicted that glial cells are also positive for MIF [78]. These findings are in accordance with our present results, as we also found strong MIF labeling in the PFC. Increasing evidence supports that the PFC is important regarding to the HPA axis, since it regulates the HPA response to stress [79], and may also play a role in the glucocorticoid feedback inhibition [80]. In our present study, MIF was predominantly found in astrocytes, and only a smaller proportion could be identified in neurons. In the Borna Disease Virus infected rat brain, accumulation of MIF in astrocyte end-feet at the blood-brain barrier was found, which correlated with reduced number of infiltrating macrophages [81]. These findings suggest that MIF in astrocytes could play a role in the modulation of the macrophage/microglia response.

However the function of MIF in the central nervous system is largely unknown, there are receptors of it, such as CD44, CD74, CXCR2 and CXCR4. The presence of these receptors suggest some alternative mechanism of action as they are found on neural stem/progenitor cells as well. It was shown that MIF promotes neural stem/progenitor cell

self-renewal, and the neuronal differentiation via the WNT/β-catenin pathway *in vitro* [82]. It was also revealed in cultured neurons that MIF acts as a chaperone for mutant superoxide dismutase (SOD1), and can directly inhibit this protein's misfolding, accumulation and association with mithochondria and endoplasmatic reticulum [83].

5. Conclusions

Neonatal clomipramine treatment causes depression-like symptoms as it was demonstrated in a rat model [18]. It was also supported by the behavioral testing of animals using FST [36], which results were reproduced in our current study as well. There is an immense literature of molecular changes in the rat brain underlying depression [84] and the question was open how neonatal clomipramine treatment could activate such a complex molecular network. Since there is no data about lifespan long molecular changes induced by chronic neonatal clomipramine administration in rats, we applied unbiased experimental strategy measuring protein level changes in this animal model. We predicted that clomipramine treatment of the flexible neonatal brain initiate a complex procedure including epigenetic and other brain developmental changes finally lead to depression-like phenotype in the adulthood. Therefore, we studied the endpoint of that predicted process experimentally. We can conclude that neonatally received chronic treatment with clomipramine is able to induce depression-like phenotype via changing the proteome and in turn the cellular phenotypes of cells. At the molecular level, chronic neonatal clomipramine treatment caused robust changes in the adult rat PFC, as 32 proteins' levels were significantly altered in the CLO group. These proteins are mainly related to energy metabolism, gene expression, cytoskeletal organization, and immunomodulation. Comparison with the literature suggests that many of the changed proteins have already been related to depression but we also implicated new proteins in the disease. In addition, we selected MIF for further examination,

which showed the largest increase in response to clomipramine treatment and is involved in the regulation of the HPA axis. The elevated level of MIF was confirmed and its distribution was described in prefrontal cortical astrocytes. This protein was suggested to be involved in inflammatory and stress-related processes. Thus, MIF could be an important participant of the molecular network rearranged in depression. Further studies of MIF provide a promising new line of investigations to uncover molecular mechanisms of the developmental form of depression.

Conflict of interest

The authors declare that no conflict of interest exists.

Acknowledgements

This work was supported by the National Development Agency of Hungary TÁMOP 4.2.1./B-09/1/KMR-2010-0003 (Katalin A. Kékesi, András Czurkó, Péter Baracskay and Gábor Juhász), the KTIA_NAP_13-2-2015-0003 (Gábor Juhász), the KTIA NAP_13-2-2014-0004 (Barbara Gellén, Katalin Völgyi and Árpád Dobolyi), OTKA K116538 (Árpád Dobolyi), KTIA_NAP_13-2-2014-0017 (Balázs A. Györffy) and KTIA_NAP_13-1-2013-0001 (Istvan Hernadi). Authors wish to thank Ágnes Kovács for her valuable technical contribution.

References

[1] Ustun TB, Ayuso-Mateos JL, Chatterji S, Mathers C, Murray CJ. Global burden of depressive disorders in the year 2000. Br J Psychiatry 2004;184:386-92.

[2] Lopez A, Murray C. The global burden of disease, 1990–2020. Nature Medicine 1998;4:1241-43.

[3] Association AP. Diagnostic and Statistical Manual of Mental Disorders, fifth ed. Arlington: American Psychiatric Publishing 2013.

[4] Kohler S, Cierpinsky K, Kronenberg G, Adli M. The serotonergic system in the neurobiology of depression: Relevance for novel antidepressants. J Psychopharmacol 2016;30:13-22.

[5] Chaudhury D, Liu H, Han MH. Neuronal correlates of depression. Cell Mol Life Sci 2015;72:4825-48.

[6] Hirschfeld RM. History and evolution of the monoamine hypothesis of depression. J Clin Psychiatry 2000;61 Suppl 6:4-6.

[7] Ruhé H, Mason N, Schene A. Mood is indirectly related to serotonin, norepinephrine and dopamine levels in humans: a meta-analysis of monoamine depletion studies. Molecular Psychiatry 2007;12:331-59.

[8] Schatzberg A, Nemeroff C. The American Psychiatric Publishing Textbook of Psychopharmacology, fourth ed. Arlington: American Psychiatric Publishing Inc; 2009.

[9] Pittenger C, Duman RS. Stress, depression, and neuroplasticity: a convergence of mechanisms. Neuropsychopharmacology 2008;33:88-109.

[10] Young J, Bruno D, Pomara N. A review of the relationship between proinflammatory cytokines and major depressive disorder. Journal of Affective Disorders 2014;169:15-20.

[11] Bloom J, Al-Abed Y. MIF: mood improving/inhibiting factor? J Neuroinflammation 2014;11:11.

[12] Dantzer R, O'Connor J, Freund G, Johnson R, Kelley K. From inflammation to sickness and depression: when the immune system subjugates the brain. Nat Rev Neurosci 2008;9:45-56.

[13] Canli T. Reconceptualizing major depressive disorder as an infectious disease. Biol Mood Anxiety Disord 2014;4:10.

[14] Jackowski A, Araújo Filho G, Almeida A, Araújo C, Reis M, Nery F, Batista I, Silva I, Lacerda A. The involvement of the orbitofrontal cortex in psychiatric disorders: an update of neuroimaging findings. Rev Bras Psiquiatr 2012;34:207-12.

[15] Koenigs M, Grafman J. The functional neuroanatomy of depression: distinct roles for ventromedial and dorsolateral prefrontal cortex. Behav Brain Res 2009;201:239-43.

[16] Nestler EJ, Barrot M, DiLeone RJ, Eisch AJ, Gold SJ, Monteggia LM. Neurobiology of depression. Neuron 2002;34:13-25.

[17] Vogel G, Vogel F. A new animal model of endogenous depression. Sleep Research 1982;11:222a.

[18] Vogel G, Neill D, Hagler M, Kors D. A new animal model of endogenous depression: a summary of present findings. Neurosci Biobehav Rev 1990;14:85-91.

[19] Mirmiran M, van de Poll N, Corner M, van Oyen H, Bour H. Suppression of active sleep by chronic treatment with chlorimipramine during early postnatal development: effects upon adult sleep and behavior in the rat. Brain Res 1981;204:129-46.

[20] Chang CH, Chen MC, Qiu MH, Lu J. Ventromedial prefrontal cortex regulates depressive-like behavior and rapid eye movement sleep in the rat. Neuropharmacology 2014;86:125-32.

[21] Limon-Morales O, Soria-Fregozo C, Arteaga-Silva M, Vazquez-Palacios G, Bonilla-Jaime H. Altered expression of 5-HT1A receptors in adult rats induced by neonatal treatment with clomipramine. Physiol Behav 2014;124:37-44.

[22] Feng P, Huang C. Phospholipase D-mTOR signaling is compromised in a rat model of depression. Journal of Psychiatric Research 2013;47:579-85.

[23] Kovacs Z, Czurko A, Kekesi KA, Juhasz G. Clomipramine increases the incidence and duration of spike-wave discharges in freely moving WAG/Rij rats. Epilepsy Res 2010;90:167-70.

[24] Maciag D, Simpson K, Coppinger D, Lu Y, Wang Y, Lin R, Paul I. Neonatal antidepressant exposure has lasting effects on behavior and serotonin circuitry. Neuropsychopharmacology 2006;31:47-57.

[25] Mayberg HS. Limbic-cortical dysregulation: a proposed model of depression. J Neuropsychiatry Clin Neurosci 1997;9:471-81.

[26] George M, Ketter T, Robert M. Prefrontal cortex dysfunction in clinical depression. Depression 1994:59-72.

[27] Kokras N, Antoniou K, Dalla C, Bekris S, Xagoraris M, Ovestreet DH, Papadopoulou-Daifoti Z. Sex-related differential response to clomipramine treatment in a rat model of depression. J Psychopharmacol 2009;23:945-56.

[28] Cryan JF, Markou A, Lucki I. Assessing antidepressant activity in rodents: recent developments and future needs. Trends Pharmacol Sci 2002;23:238-45.

[29] Cryan J, Valentino R, Lucki I. Assessing substrates underlying the behavioral effects of antidepressants using the modified rat forced swimming test. Neurosci Biobehav Rev 2005:547-69.

[30] Porsolt RD, Bertin A, Jalfre M. Behavioral despair in mice: a primary screening test for antidepressants. Arch Int Pharmacodyn Ther 1977;229:327-36.

[31] Liu J, Pu C, Lang L, Qiao L, Abdullahi MA, Jiang C. Molecular pathogenesis of hereditary hemochromatosis. Histol Histopathol 2016:11762.

[32] Szego EM, Janaky T, Szabo Z, Csorba A, Kompagne H, Muller G, Levay G, Simor A, Juhasz G, Kekesi KA. A mouse model of anxiety molecularly characterized by altered protein networks in the brain proteome. Eur Neuropsychopharmacol 2010;20:96-111.

[33] Marouga R, David S, Hawkins E. The development of the DIGE system: 2D fluorescence difference gel analysis technology. Anal Bioanal Chem 2005:669-78.

[34] Santos-Gonzalez M, Gomez Diaz C, Navas P, Villalba JM. Modifications of plasma proteome in long-lived rats fed on a coenzyme Q10-supplemented diet. Exp Gerontol 2007;42:798-806.

[35] Bonilla-Jaime H, Retana-Marquez S, Velazquez-Moctezuma J. Pharmacological features of masculine sexual behavior in an animal model of depression. Pharmacol Biochem Behav 1998;60:39-45.

[36] Velazquez-Moctezuma J, Diaz Ruiz O. Neonatal treatment with clomipramine increased immobility in the forced swim test: an attribute of animal models of depression. Pharmacol Biochem Behav 1992;42:737-9.

[37] Mallei A, Giambelli R, Gass P, Racagni G, Mathe AA, Vollmayr B, Popoli M. Synaptoproteomics of learned helpless rats involve energy metabolism and cellular remodeling pathways in depressive-like behavior and antidepressant response. Neuropharmacology 2011;60:1243-53.

[38] Beasley CL, Pennington K, Behan A, Wait R, Dunn MJ, Cotter D. Proteomic analysis of the anterior cingulate cortex in the major psychiatric disorders: Evidence for disease-associated changes. Proteomics 2006;6:3414-25.

[39] Katyare SS, Rajan RR. Effect of long-term in vivo treatment with imipramine on the oxidative energy metabolism in rat brain mitochondria. Comp Biochem Physiol C Pharmacol Toxicol Endocrinol 1995;112:353-7.

[40] Gardner A, Boles RG. Beyond the serotonin hypothesis: mitochondria, inflammation and neurodegeneration in major depression and affective spectrum disorders. Prog Neuropsychopharmacol Biol Psychiatry 2011;35:730-43.

[41] Kambe Y, Miyata A. Potential involvement of the mitochondrial unfolded protein response in depressive-like symptoms in mice. Neurosci Lett 2015;588:166-71.

[42] Segal M, Avital A, Drobot M, Lukanin A, Derevenski A, Sandbank S, Weizman A. Serum creatine kinase level in unmedicated nonpsychotic, psychotic, bipolar and schizoaffective depressed patients. Eur Neuropsychopharmacol 2007;17:194-8.

[43] Feier G, Valvassori SS, Rezin GT, Burigo M, Streck EL, Kapczinski F, Quevedo J. Creatine kinase levels in patients with bipolar disorder: depressive, manic, and euthymic phases. Rev Bras Psiquiatr 2011;33:171-5.

[44] Santos P, Scaini G, Rezin G, Benedet J, Rochi N, Jeremias G, Carvalho-Silva M, Quevedo J, Streck E. Brain creatine kinase activity is increased by chronic administration of paroxetine. Brain Res Bull 2009;80:327-30.

[45] MacDonald ML, Naydenov A, Chu M, Matzilevich D, Konradi C. Decrease in creatine kinase messenger RNA expression in the hippocampus and dorsolateral prefrontal cortex in bipolar disorder. Bipolar Disord 2006;8:255-64.

[46] Gawryluk JW, Wang JF, Andreazza AC, Shao L, Yatham LN, Young LT. Prefrontal cortex glutathione S-transferase levels in patients with bipolar disorder, major depression and schizophrenia. Int J Neuropsychopharmacol 2011;14:1069-74.

[47] Wang J, Shao L, Sun X, Young L. Glutathione S-transferase is a novel target for mood stabilizing drugs in primary cultured neurons. J Neurochem 2004;88:1477-84.

[48] Shao L, Cui J, Young LT, Wang JF. The effect of mood stabilizer lithium on expression and activity of glutathione s-transferase isoenzymes. Neuroscience 2008;151:518-24.

[49] Baxter LR, Jr., Schwartz JM, Phelps ME, Mazziotta JC, Guze BH, Selin CE, Gerner RH, Sumida RM. Reduction of prefrontal cortex glucose metabolism common to three types of depression. Arch Gen Psychiatry 1989;46:243-50.

[50] Kennedy S, Evans K, Krüger S, Mayberg H, Meyer J, McCann S, Arifuzzman A, Houle S, Vaccarino F. Changes in regional brain glucose metabolism measured with positron emission tomography after paroxetine treatment of major depression. Am J Psychiatry 2001;158:899-905.

[51] Messaoudi E, Kanhema T, Soulé J, Tiron A, Dagyte G, da Silva B, Bramham C. Sustained Arc/Arg3.1 synthesis controls long-term potentiation consolidation through regulation of local actin polymerization in the dentate gyrus in vivo. J Neurosci 2007;27:10445-55.

[52] Li Y, Pehrson A, Waller J, Dale E, Sanchez C, Gulinello M. A critical evaluation of the activity-regulated cytoskeleton-associated protein (Arc/Arg3.1)'s putative role in regulating dendritic plasticity, cognitive processes, and mood in animal models of depression. Front Neurosci 2015;9:279.

[53] Piubelli C, Vighini M, Mathe AA, Domenici E, Carboni L. Escitalopram modulates neuron-remodelling proteins in a rat gene-environment interaction model of depression as revealed by proteomics. Part I: genetic background. Int J Neuropsychopharmacol 2011;14:796-833.

[54] Bianchi M, Heidbreder C, Crespi F. Cytoskeletal changes in the hippocampus following restraint stress: role of serotonin and microtubules. Synapse 2003;49:188-94.

[55] Yang C, Wang G, Wang H, Liu Z, Wang X. Cytoskeletal alterations in rat hippocampus following chronic unpredictable mild stress and re-exposure to acute and chronic unpredictable mild stress. Behav Brain Res 2009;205:518-24.

[56] Bianchi M, Fone KF, Azmi N, Heidbreder CA, Hagan JJ, Marsden CA. Isolation rearing induces recognition memory deficits accompanied by cytoskeletal alterations in rat hippocampus. Eur J Neurosci 2006;24:2894-902.

[57] Bianchi M, Shah AJ, Fone KC, Atkins AR, Dawson LA, Heidbreder CA, Hows ME, Hagan JJ, Marsden CA. Fluoxetine administration modulates the cytoskeletal microtubular system in the rat hippocampus. Synapse 2009;63:359-64.

[58] Wong GT, Chang RC, Law AC. A breach in the scaffold: the possible role of cytoskeleton dysfunction in the pathogenesis of major depression. Ageing Res Rev 2013;12:67-75.

[59] Vlachos I, Barbatis C, Tsopanomichalou M, Abou-Assabeh L, Goumas K, Ginieri-Coccossis M, Economou M, Papadimitriou G, Patsouris E, Nicolopoulou-Stamati P. Correlation between depression, anxiety, and polymorphonuclear cells' resilience in ulcerative colitis: the mediating role of heat shock protein 70. BMC Gastroenterol 2014;14:77.

[60] Pae CU, Mandelli L, Serretti A, Patkar AA, Kim JJ, Lee CU, Lee SJ, Lee C, De Ronchi D, Paik IH. Heat-shock protein-70 genes and response to antidepressants in major depression. Prog Neuropsychopharmacol Biol Psychiatry 2007;31:1006-11.

[61] Martins-de-Souza D, Guest PC, Harris LW, Vanattou-Saifoudine N, Webster MJ, Rahmoune H, Bahn S. Identification of proteomic signatures associated with depression and psychotic depression in post-mortem brains from major depression patients. Transl Psychiatry 2012;2:e87.

[62] Muller N, Schwarz MJ. The immune-mediated alteration of serotonin and glutamate: towards an integrated view of depression. Mol Psychiatry 2007;12:988-1000.

[63] Gibney SM, Drexhage HA. Evidence for a dysregulated immune system in the etiology of psychiatric disorders. J Neuroimmune Pharmacol 2013;8:900-20.

[64] Savaskan NE, Fingerle-Rowson G, Buchfelder M, Eyupoglu IY. Brain miffed by macrophage migration inhibitory factor. Int J Cell Biol 2012;2012:139573.

[65] Kohler O, Benros ME, Nordentoft M, Farkouh ME, Iyengar RL, Mors O, Krogh J. Effect of anti-inflammatory treatment on depression, depressive symptoms, and adverse effects: a systematic review and meta-analysis of randomized clinical trials. JAMA Psychiatry 2014;71:1381-91.

[66] Bick J, Nguyen V, Leng L, Piecychna M, Crowley M, Bucala R, Mayes L, Grigorenko E. Preliminary associations between childhood neglect, MIF, and cortisol: potential pathways to long-term disease risk. Dev Psychobiol 2015;57:131-9.

[67] Edwards K, Bosch J, Engeland C, Cacioppo J, Marucha P. Elevated macrophage migration inhibitory factor (MIF) is associated with depressive symptoms, blunted cortisol reactivity to acute stress, and lowered morning cortisol. Brain Behav Immun 2010;24:1202-8.

[68] Katsuura S, Kamezaki Y, Tominaga K, Masuda K, Nishida K, Yamamoto Y, Takeo K, Yamagishi N, Tanahashi T, Kawai T, Rokutan K. High-throughput screening of brief naturalistic stress-responsive cytokines in university students taking examinations. Int J Psychophysiol 2010;77:135-40.

[69] Rohleder N, Wolf JM, Wolf OT. Glucocorticoid sensitivity of cognitive and inflammatory processes in depression and posttraumatic stress disorder. Neurosci Biobehav Rev 2010;35:104-14.

[70] Raison C, Miller A. When not enough is too much: the role of insufficient glucocorticoid signaling in the pathophysiology of stress-related disorders. Am J Psychiatry 2003;160:1554-65.

[71] Pace TW, Miller AH. Cytokines and glucocorticoid receptor signaling. Relevance to major depression. Ann N Y Acad Sci 2009;1179:86-105.

[72] Aeberli D, Leech M, Morand E. Macrophage migration inhibitory factor and glucocorticoid sensitivity. Rheumatology (Oxford) 2006;45:937-43.

[73] Pariante CM, Pearce BD, Pisell TL, Sanchez CI, Po C, Su C, Miller AH. The proinflammatory cytokine, interleukin-1alpha, reduces glucocorticoid receptor translocation and function. Endocrinology 1999;140:4359-66.

[74] Prathiba J, Kumar KB, Karanth KS. Hyperactivity of hypothalamic pituitary axis in neonatal clomipramine model of depression. J Neural Transm (Vienna) 1998;105:1335-9.

[75] Holsboer-Trachsler E, Stohler R, Hatzinger M. Repeated administration of the combined dexamethasone-human corticotropin releasing hormone stimulation test during treatment of depression. Psychiatry Res 1991;38:163-71.

[76] Nemeroff CB. The role of corticotropin-releasing factor in the pathogenesis of major depression. Pharmacopsychiatry 1988;21:76-82.

[77] Kostadinov I, Delev D, Petrova A, Stanimirova I, Draganova K, Kostadinova I, Murdjeva M. Study on anti-inflammatory and immunomodulatory effects of clomipramine in carrageenan- and lipopolysaccharide-induced rat models of inflammation. Biotechnol Biotechnol Equip 2014;28:552-8.

[78] Bacher M, Meinhardt A, Lan HY, Dhabhar FS, Mu W, Metz CN, Chesney JA, Gemsa D, Donnelly T, Atkins RC, Bucala R. MIF expression in the rat brain: implications for neuronal function. Mol Med 1998;4:217-30.

[79] Kern S, Oakes TR, Stone CK, McAuliff EM, Kirschbaum C, Davidson RJ. Glucose metabolic changes in the prefrontal cortex are associated with HPA axis response to a psychosocial stressor. Psychoneuroendocrinology 2008;33:517-29.

[80] Smith SM, Vale WW. The role of the hypothalamic-pituitary-adrenal axis in neuroendocrine responses to stress. Dialogues Clin Neurosci 2006;8:383-95.

[81] Bacher M, Weihe E, Dietzschold B, Meinhardt A, Vedder H, Gemsa D, Bette M. Borna disease virus-induced accumulation of macrophage migration inhibitory factor in rat brain astrocytes is associated with inhibition of macrophage infiltration. Glia 2002;37:291-306.

[82] Zhang X, Chen L, Wang Y, Ding Y, Peng Z, Duan L, Ju G, Ren Y, Wang X. Macrophage migration inhibitory factor promotes proliferation and neuronal differentiation of neural stem/precursor cells through Wnt/β-catenin signal pathway. Int J Biol Sci 2013;9:1108-20.

[83] Israelson A, Ditsworth D, Sun S, Song S, Liang J, Hruska-Plochan M, McAlonis-Downes M, Abu-Hamad S, Zoltsman G, Shani T, Maldonado M, Bui A, Navarro M, Zhou H, Marsala M, Kaspar B, Da Cruz S, Cleveland D. Macrophage migration inhibitory factor as a chaperone inhibiting accumulation of misfolded SOD1. Neuron 2015;86:218-32.

[84] Lang UE, Borgwardt S. Molecular mechanisms of depression: perspectives on new treatment strategies. Cell Physiol Biochem 2013;31:761-77.

Figure and Table legends

Figure 1. Graphs of the forced swim test results of the full cohort. The white columns represent the control (C), while the grey columns the clomipramine treated animals (CLO). The average time spent in each behavioral category is shown. Significant changes were found in the floating ($p < 0.001$) and struggling ($p < 0.05$) categories between the two groups. Mean ± SEM is shown. * $p < 0.05$, *** $p < 0.001$.

Figure 2. Representative 2D-DIGE image of the gel with the location of numbered, significantly altered protein spots (n = 24). Red circles indicate increased protein level in the clomipramine treated group, while the blue color represents decreased proteins.

Figure 3. Functional clustering of the significant protein changes according to UniProt database. Each protein is clustered in one group only, which represents its most relevant function.

Figure 4. The cellular localization of the significantly changed proteins in the plasma membrane, mitochondrion, cytosol and nucleus. The shapes indicate the number of cellular locations a particular protein belongs to as follows: the oval indicates proteins in one, the rectangle in two, and the hexagon in three known localizations in different cellular compartments. Red and blue colors highlight proteins with increased and decreased levels, respectively.

Figure 5. Common regulator (A) and target (B) analysis of significantly altered proteins, focusing on MIF connections.

Common regulators: AGT – angiotensinogen, CABPA – CAAT/enhancer binding protein alpha, CREB1 – cyclic AMP-responsive element-binding protein 1, DPYSL-2 – dihydropyrimidinase-related protein 2, EDN1 – endothelin-1, GAPDH – glyceraldehyde-3-phosphate dehydrogenase, GSTA-2 – glutathione S-transferase alpha-2, HIF1A – hypoxia-

inducible factor 1-alpha, HOMER1 – homer protein homolog 1, HSPA8 – heat shock cognate 71 kDa protein, IL1-B – interleukin-1 beta, INS – insulin, MAPK1 – mitogen-activated protein kinase 1, MIF – macrophage migration inhibitory factor, PGK1 – phosphoglycerate kinase 1, SP1 – transcription factor Sp1, TNF – tumor necrosis factor, TPI1 – triosephosphate isomerase, TXN – thioredoxin.

Common targets: AGTR1 – type-1A angiotensin II receptor, BCL2 – apoptosis regulator Bcl-2, CCL2 – C-C motif chemokine 2, CCND1 – G1/S-specific cyclin-D1, CD40LG – CD40 ligand, CDKN1B – cyclin-dependent kinase inhibitor 1B, FOS – proto-oncogene c-Fos, HIF1A – hypoxia-inducible factor 1-alpha, IFNG – interferon gamma, IL1B – interleukin-1 beta, IL2 – interleukin-2, IL2R – interleukin-2 receptor, IL2RA – interleukin-2 receptor subunit alpha, IL4 – interleukin-4, IL6 – interleukin-6, IL8 – interleukin-8, IL12 – interleukin-12 subunit beta, IL13 – interleukin-13, MMP2 – 72 kDa type IV collagenase, MMP3 – stromelysin-1, NFKB1A – NF-kappa-B inhibitor alpha, NR3C1 – glucocorticoid receptor, PTGS2 – prostaglandin G/H synthase 2, TGFB1 – transforming growth factor beta-1, TNF – tumor necrosis factor, TP53 – cellular tumor antigen p53, VEGFA – vascular endothelial growth factor A.

Figure 6. Validation of the increased protein level of MIF in the clomipramine-treated (CLO) group with Western blot. The MIF immunopositive band is shown at 12.5 kDa. A 1.63 ± 0.52-fold increase ($p = 0.038$) in CLO group was revealed in comparison with controls (C) ($n = 4$ per group) using densitometric analysis. Mean ± SEM is shown. * $p < 0.05$

Figure 7. Distribution of the MIF-immunoreactivity (ir) in the prefrontal cortex (PFC). Aa: The low-magnification image shows double labeling with the neuronal marker NeuN (red) which demonstrates different distributional pattern with MIF-ir cells (green) being most abundant in the upper layers where only few neurons are located. Ab: The high-magnification image demonstrates the lack of colocalization between MIF and NeuN. Ba: MIF (green) and

the astrocyte marker S100 (red) have similar distributions in all layers of the PFC. Bb: The high-magnification image demonstrates a high degree of colocalization between MIF- and S100-ir cells. Scale bars: Aa and Ba: 500 μm, Ab and Bb: 100 μm.

Table 1. Significantly increased proteins in the clomipramine treated group in comparison with controls. Abbreviations: Acc: accession number, AR: average ratio, SC%: sequence coverage percentage. The cellular location, molecular function, and biological process related to the proteins were also described.

Table 2. Significantly decreased proteins in the clomipramine treated group in comparison with controls. Abbreviations: Acc: accession number, AR: average ratio, SC%: sequence coverage percentage. The cellular location, molecular function, and biological process related to the proteins were also described.

Figure 1

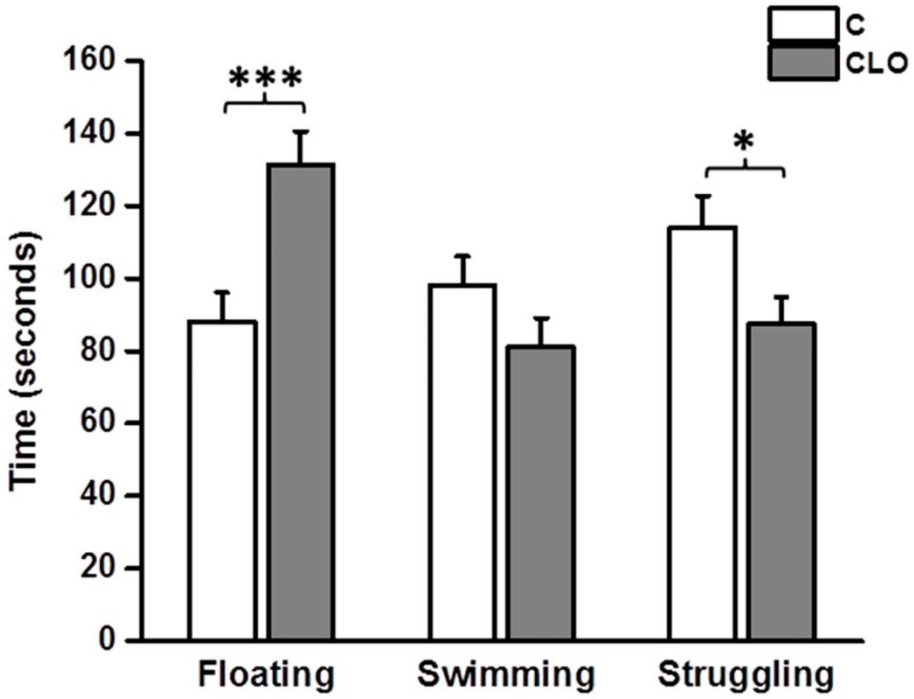

Figure 2

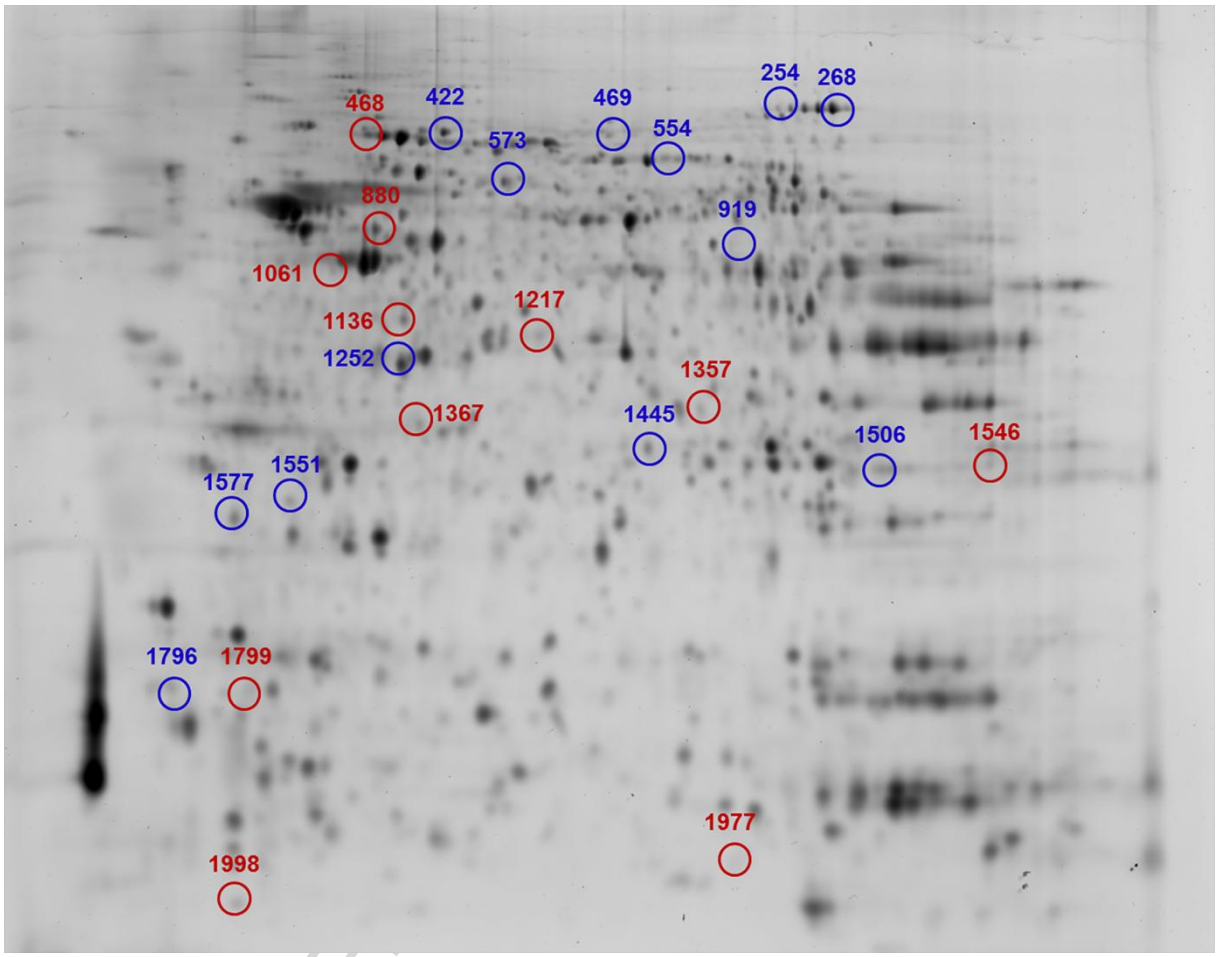

Figure 3

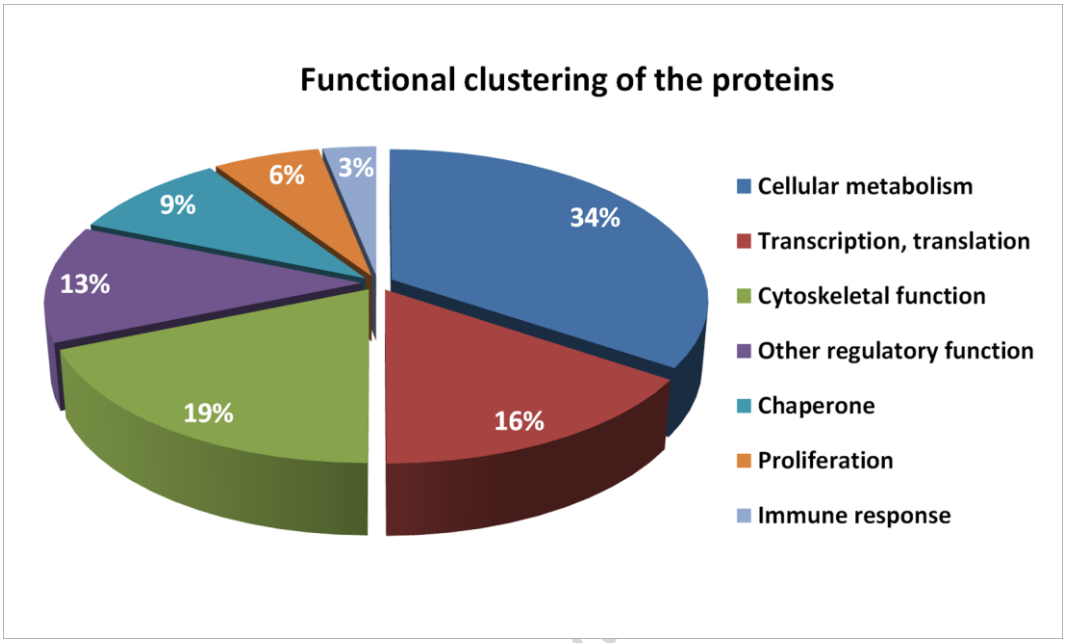

Figure 4

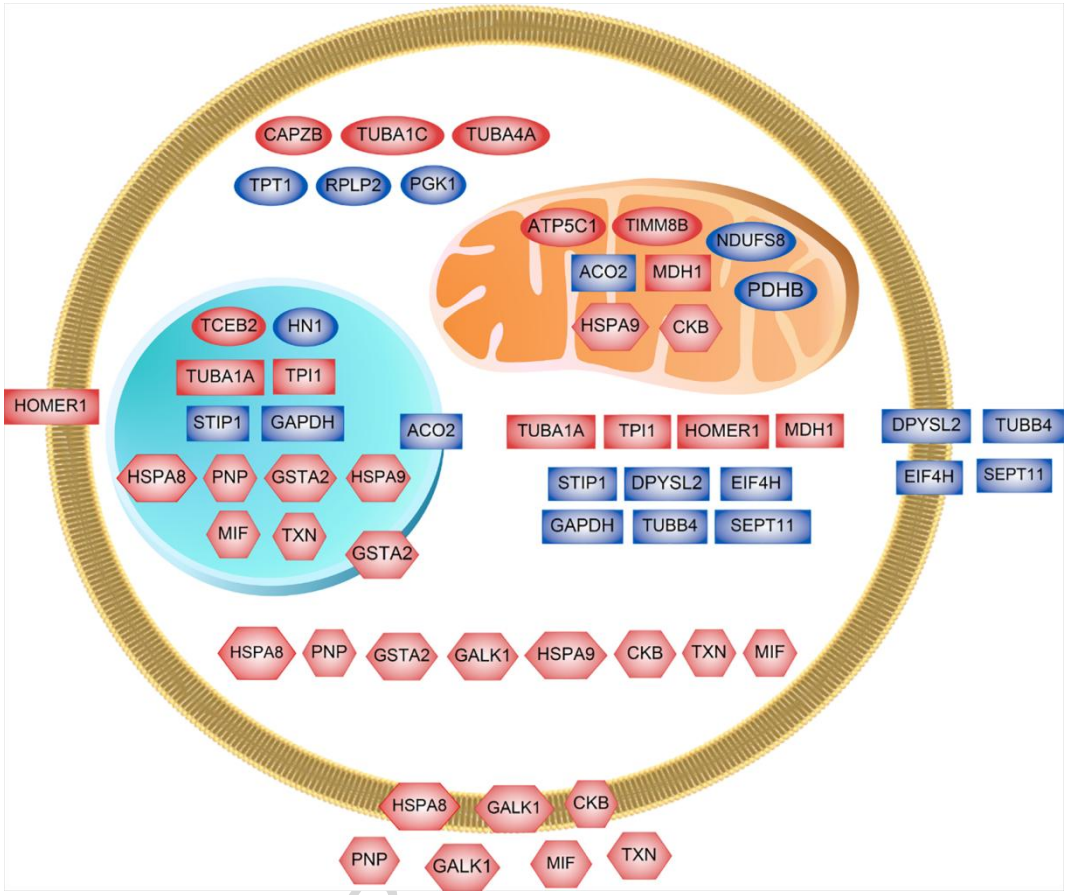

Figure 5

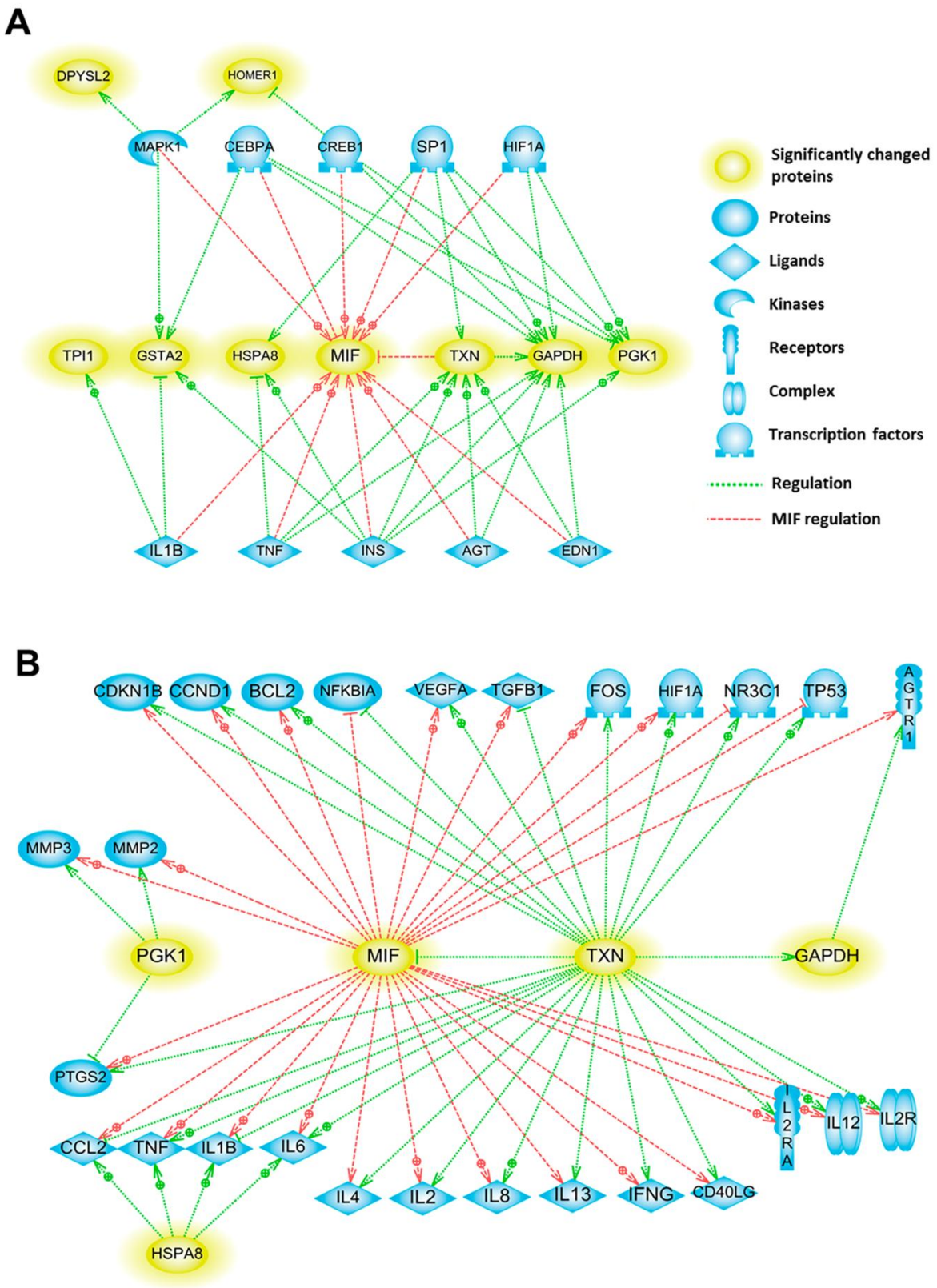

Figure 6

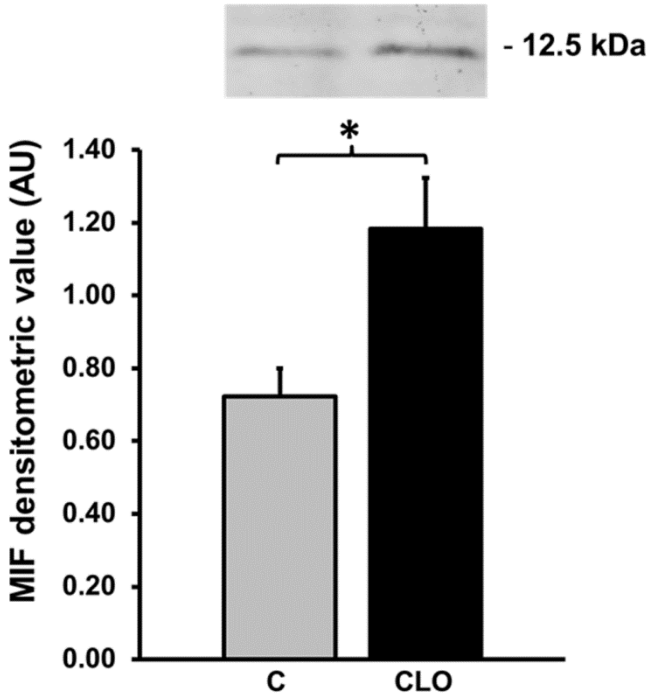

Figure 7

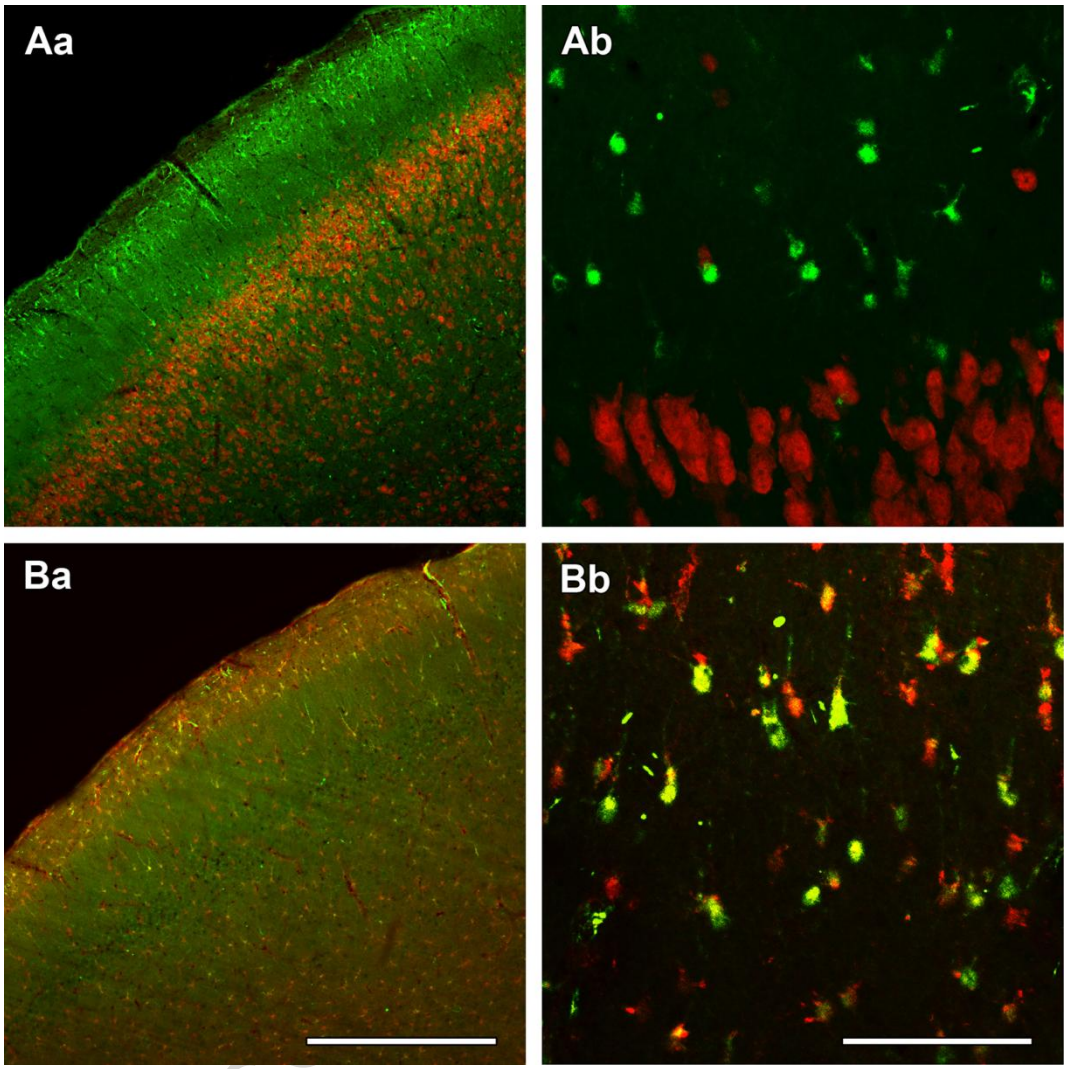

Table 1

Spot No.	Acc	Gene	Protein name	AR	p-value	SC%	Unique peptides	Location	Molecular function	Biological process
1977	P30904	MIF	Macrophage migration inhibitory factor	1.65	0.004	41	5	Cytoplasm, Extracellular, Nucleus	Cytokine, Isomerase	Immunity, Inflammatory response, Innate immunity
468	Q9Z214	HSPA8	Heatshock 70 kDa protein 8	1.43	0.041	16	7	Cytoplasm, Membrane, Nucleus	Chaperone, Repressor	Transcription, Transcription regulation, Stress response, mRNA processing, Splicing
1367	Q5XI32	CAPZB	F-actin-capping protein subunit beta	1.37	0.021	20	6	Cytoplasm	Actin capping	Cytoskeleton organization, Neuron projection development, Regulation of cell morphogenesis
1367	P35435	ATP5C1	ATP synthase, H+ transporting, mitochondrial F1 complex, gamma polypeptide 1	1.37	0.021	8	2	Mitochondria	Proton transporting, ATPase, synthase activity	ATP synthesis, Hydrogen ion transport, Ion transport
1998	P62078	TIMM8	Translocase of inner mitochondrial membrane 8 homolog B	1.32	0.013	26	2	Mitochondria	Chaperone	Protein import
1998	P11232	TXN	Thioredoxin	1.32	0.013	22	3	Cytoplasm, Extracellular, Nucleus	Activator	Transport, Electron transport, Transcription regulation
1136	P68370	TUBA1A	Tubulin, alpha 1 a	1.28	0.034	6	3	Cytoplasm, Nucleus	GTPase activity, Structural constituent of cytoskeleton	Microtubule based process, Protein polymerization
1136	Q6AYZ1	TUBA1C	Tubulin, alpha 1 c	1.28	0.034	10	3	Cytoplasm	GTPase activity, Structural constituent of cytoskeleton	Microtubule based process, Protein polymerization
1136	Q5XIF6	TUBA4A	Tubulin, alpha 4 a	1.28	0.034	10	3	Cytoplasm	GTPase activity, Structural constituent of cytoskeleton	Microtubule based process, Protein polymerization
1546	P48500	TPI1	Triosephosphate isomerase 1	1.25	0.009	16	3	Cytoplasm, Nucleus	Isomerase	Gluconeogenesis, Glycolysis, Pentose shunt

1546	P04903	GSTA2	GlutathioneS-transferase A2	1.25	0.009	17	4	Cytoplasm, Membrane, Nucleus	Glutathione transferase activity, Drug binding	Aging, Xenobiotic catabolic process, Detoxification
1799	P62870	TCEB2	Transcription elongation factor B (SIII), polypeptide 2 (18 kDa, elongin B)	1.24	0.046	27	4	Nucleus	Protein complex binding, Transcription coactivator activity	Transcription, Transcription regulation, Ubl conjugation pathway
1061	Q5RKH2	GALK1	Galactokinase 1	1.11	0.043	27	8	Cytoplasm, Membrane, Extracellular	Kinase	Carbohydrate phosphorylation, Galactose metabolic process
1217	O88989	MDH1	Malate dehydrogenase 1	1.19	0.015	5	2	Cytoplasm, Mitochondria	Oxidoreductase	Tricarboxylic acid cycle
1217	Q566Q8	Bles03	UPF0696 protein C11orf68 homolog	1.19	0.015	11	2	NA	NA	NA
1357	P85973	NP	Nucleoside phosphorylase	1.18	0.044	10	2	Cytoplasm, Extracellular, Nucleus	Glycosyltransferase, Transferase	Purine nucleoside metabolic process
880	Q9Z214	HOMER1	Homer protein homolog 1	1.17	0.041	23	7	Cytoplasm, Membrane	Receptor, Scaffold protein binding, Protein complex	Protein localization to synapse, Response to calcium
880	P07335	CKB	Creatine kinase	1.17	0.041	39	9	Cytoplasm, Mitochondria, Membrane	Kinase, Transferase	Phosphocreatine metabolic process, Cellular chloride ion homeostasis

Table 2

Spot No.	Acc	Gene	Protein name	AR	p-value	SC%	Unique peptides	Location	Molecular function	Biological process
919	P16617	PGK1	Phosphoglycerate kinase 1	-1.34	0.040	11	3	Cytoplasm	Kinase, Transferase	Glycolysis
919	B3GNI6	SEPT11	Septin 11	-1.34	0.040	7	2	Cytoplasm, Extracellular	GTP binding	Cell cycle, Cell division
254	Q9ER34	ACO2	Aconitase 2	-1.33	0.041	30	19	Mitochondria, Nucleus	Lyase	Tricarboxylic acid cycle
268				-1.19	0.048	30	22			
1551	B0BNE6	NDUFS8	NADH dehydrogenase Fe-S protein 8 (predicted)	-1.23	0.011	20	5	Mitochondria	NADH dehydrogenase activity	Mitochondrial respiratory chain complex I assembly
1551	Q6AXU6	HN1	Hematological and neurological expressed 1	-1.23	0.011	19	2	Nucleus	NA	Developmental process
469	P47942	DPYSL2	Dihydropyrimidinase-like 2	-1.21	0.037	6	3	Cytoplasm, Membrane	Hydrolase	Differentiation, Neurogenesis
554				-1.16	0.005	22	10			
573				-1.13	0.020	9	4			
1445	Q5XI72	EIFH4	Eukaryotic translation initiation factor 4H	-1.18	0.043	14	3	Cytoplasm, Membrane	Protein synthesis	Translation
554	O35814	STIP1	Stress-induced-phosphoprotein (Hsp70/Hsp90-organizing protein)	-1.16	0.005	4	2	Cytoplasm, Nucleus	Chaperone binding	Response to stress
1796	P02401	RPLP2	Ribosomal protein, large, P2	-1.15	0.039	50	7	Cytoplasm	Structural constituent of ribosome	Translation elongation

1506	P04797	GAPDH	Glyceraldehyde-3-phosphate dehydrogenase	-1.11	0.009	15	3	Cytoplasm, Nucleus	Oxydoreductase, Transferase	Apoptosis, Glycolysis, Translation regulation
1577	P63029	TPT1	Tumor protein translationally-controlled 1	-1.1	0.027	34	7	Cytoplasm	Ca binding – Microtubule stabilization	Cell proliferation, Spermatogenesis
1252	B4F7C2	TUBB4	Tubulin, beta 4/5	-1.1	0.038	19	6	Cytoplasm, Extracellular	GTPase activity, Structural constituent of cytoskeleton	Microtubule based process, Protein polymerization
1252	P49432	PDHB	Pyruvate dehydrogenase (lipoamide) beta	-1.1	0.038	38	14	Mitochondria	Oxidoreductase	Carbohydrate, Glucose metabolism, Tricarboxylic acid
422	P48721	HSPA9	Heatshock 70 kDa protein 9 (mortalin)	-1.08	0,009	34	4	Cytoplasm, Mitochondria, Nucleus	Chaperone	ATP-binding, Nucleotide-binding

Conflict of interest

The authors declare that no conflict of interest exists.

Graphical abstract

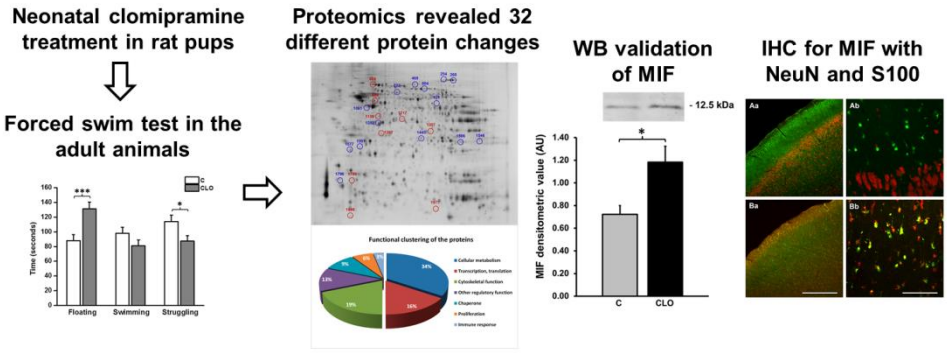

Highlights

- Chronic neonatal clomipramine treatment induces depression-like symptoms in rats
- Altered levels of 32 proteins have been revealed in the prefrontal cortex of rats
- The macrophage migration inhibitory factor (MIF) showed the largest alteration
- MIF is predominantly expressed in astrocytes
- Inflammation-associated mechanisms are suggested in this model